

## Article

# Analysis of Growth Characteristics of Kimchi Cabbage Using Drone-Based Cabbage Surface Model Image

Seung-Hwan Go <sup>1</sup>, Dong-Ho Lee <sup>1</sup>, Sang-Il Na <sup>2</sup> and Jong-Hwa Park <sup>1,\*</sup>

<sup>1</sup> Department of Agricultural and Rural Engineering, Chungbuk National University, 1 Chungdae-ro, Seowon-gu, Cheongju 28644, Chungbuk, Korea; shgo916@chungbuk.ac.kr (S.-H.G.); ehdgh3337@naver.com (D.-H.L.)

<sup>2</sup> National Institute of Agricultural Sciences, 166, Nongsaengmyeong-ro, Iseo-myeon, Wanju 55365, Jeollabuk-do, Korea; sangil917@korea.kr

\* Correspondence: jhpak7@cbnu.ac.kr; Tel.: +82-43-261-2577

**Abstract:** Cultivation soil is the basis for cabbage growth, and it is important to assess not only to provide information on how it affects the growth of vegetable crops but also for cultivation management. Until now, field cabbage surveys have measured size and growth variations in the field, and this method requires a lot of time and effort. Drones and sensors provide opportunities to accurately capture and utilize cabbage growth and variation data. This study aims to determine the growth stages based on drone remote estimation of the cabbage height and evaluate the impact of the soil texture on cabbage height. Time series variation according to the growth of Kimchi cabbage exhibits an S-shaped sigmoid curve. The logistic model of the growth curve indicates the height and growth variation of Kimchi cabbage, and the growth rate and growth acceleration formula of Kimchi cabbage can thus be derived. The curvature of the growth parameter can be used to identify variations in Kimchi cabbage height and its stages of growth. The main research results are as follows. (1) According to the growth curve, Kimchi cabbage growth can be divided into four stages: initial slow growth stage (seedling), growth acceleration stage (transplant and cupping), heading through slow growth, and final maturity. The three boundary points of the Kimchi cabbage growth curve are  $0.2113 G_{max}$ ,  $0.5 G_{max}$ , and  $0.7887 G_{max}$ , where  $G_{max}$  is the maximum height of Kimchi cabbage. The growth rate of cabbage reaches its peak at  $0.5 G_{max}$ . The growth acceleration of cabbage forms inflection points at  $0.2113 G_{max}$  and  $0.7887 G_{max}$ , and shows a variation characteristic. (2) The produced logistic growth model expresses the variation in the cabbage surface model value for each date of cabbage observation under each soil texture condition, with a high degree of accuracy. The accuracy evaluation showed that  $R^2$  was at least 0.89, and the normalized root-mean-square error ( $nRMSE$ ) was 0.09 for clay loam, 0.06 for loam, and 0.07 for sandy loam, indicating a very strong regression relationship. It can be concluded that the logistic model is an important model for the phase division of cabbage growth and height variation based on cabbage growth parameters. The results obtained in this study provide a new method for understanding the characteristics and mechanisms of the growth phase transition of cabbage, and this study will be useful in the future to extract various types of information using drones and sensors from field vegetable crops.

**Keywords:** logistic model; growth curve; growth rate; growth acceleration; drone



**Citation:** Go, S.-H.; Lee, D.-H.; Na, S.-I.; Park, J.-H. Analysis of Growth Characteristics of Kimchi Cabbage Using Drone-Based Cabbage Surface Model Image. *Agriculture* **2022**, *12*, 216. <https://doi.org/10.3390/agriculture12020216>

Academic Editor: Francesco Marinello

Received: 15 December 2021

Accepted: 29 January 2022

Published: 2 February 2022

**Publisher's Note:** MDPI stays neutral with regard to jurisdictional claims in published maps and institutional affiliations.



**Copyright:** © 2022 by the authors. Licensee MDPI, Basel, Switzerland. This article is an open access article distributed under the terms and conditions of the Creative Commons Attribution (CC BY) license (<https://creativecommons.org/licenses/by/4.0/>).

## 1. Introduction

The international pandemic situation caused by COVID-19 has exposed the problems and limitations in systems used around the world to produce and supply agricultural products. In particular, the agricultural sector often relies on manpower, but global supply chain problems, restrictions in the movement of manpower, and rising labor costs necessitate new alternatives. The growth potential of cabbage due to changes in natural conditions needs to be analyzed through field investigations. The on-site survey method, which has been most popular so far, requires a lot of manpower and time.

Chinese cabbage is mainly used as a side dish in Korea, China, and Japan, so research has focused on improving varieties [1,2], cultivation [3,4], and yield [5,6], focusing on consumption regions. Kimchi cabbage is an improved type of Chinese cabbage. In addition, as the main raw ingredient of Kimchi, Kimchi cabbage has increased in demand as interest in immune-enhancing foods has grown following COVID-19 [7,8]. Since Kimchi is mainly made from Kimchi cabbage, changes in the production and consumption of cabbage are linked not only to prices but also to farm household income. Kimchi cabbage is a vegetable with high price volatility due to natural conditions, its specific production period, and restrictions on cultivation areas [9]. In particular, the production of major vegetable crops has a great influence on consumer prices, so it is very important to predict the production before harvest and equip technology to prepare for it.

The growth of vegetables, including Kimchi cabbage, is not a uniform process of change, but a dynamic process of initial slow growth, then rapid growth, and finally slow growth [10]. Kimchi cabbage is a vegetable crop that grows for a short period of time and requires a lot of moisture, especially in the early stage of head growth [11]. The growth of Kimchi cabbage is affected by natural factors such as temperature [12], soil moisture [13], and irrigation [14] and depends on the growing season and moisture conditions. This means that cabbage growth has properties that vary in response to climatic and soil conditions [15,16]. The growth process of Kimchi cabbage shows spatial variations in the stems and leaves depending on factors related to soil, moisture, and temperature. The growth characteristics of vegetable crops such as Kimchi cabbage can be determined via changes in size, height, vegetation index, leaf area, and other factors [11].

Agricultural observation requires the establishment of a scientific observation system for periodically identifying and presenting vegetables that are diversely distributed in a wide area, as well as analyzing their characteristics. The head size and height of Kimchi cabbage are basic measures that can reflect the growth stage of Kimchi cabbage [17]. Unfortunately, it is not easy to obtain reliable data when the head sizes of Kimchi cabbage are spread over a large-scale cultivation area.

Another approach is to use remote sensing (RS) images to derive spatial information from cultivated fields. There have been many examples of the application of RS technology in agriculture since the 1980s when Landsat and MODIS satellite imageries were used [18]. However, most of the measurements of crop growth and yield [19] have been conducted on major crops such as rice [20,21], wheat [22], corn [23], and soybean [24].

Drone and sensor technologies are rapidly developing and being introduced into agricultural observation practices to increase their usability [25,26]. In agricultural observation, it is very important to accurately analyze the growth characteristics of each vegetable crop and to manage cultivation through the minimum input of manpower [27]. Observation accuracy is increasing as a result of using spatial information in a scientific way. However, even in drone research, in many countries, cultivation area identification and quantity prediction have mainly centered on the world's four major crops [28–31].

It is important to manage the cultivation of Kimchi cabbage to satisfy quality and price conditions, and this can be carried out by adjusting the harvest time according to local conditions, such as those related to soil and moisture. Research on the growth potential of Kimchi cabbage has been mainly conducted in South Korea and has not involved the production of a growth estimation model using drones and the main factors of the productivity of vegetable crops [32].

Field-grown vegetable crops grow differently depending on the soil conditions in which they are planted [33]. The difference in drainage makes the moisture content of each soil different. However, there are not many studies on the effect of field soil characteristics on cabbage growth [5,34]. The growth dependence of Kimchi cabbage is affected by the soil texture conditions of the cultivation area, and these can be identified through the spatial analysis of images. Drone and sensor measurement images are some of the most powerful tools for analyzing the conditions of different cultivation environments. Drones are effective in monitoring the growth of Kimchi cabbage because they can acquire high-resolution

image data anytime and anywhere [35]. In particular, when monitoring Kimchi cabbage, the cabbage surface model (CSM) derived using the digital surface model (DSM) is suitable for obtaining data on the height growth of crops. The growth process of Kimchi cabbage is an indicator of the spatial distribution and variation of cabbage [27].

The logistic growth curve can be used to explain the growth process of a biological object [34,36]. In general, a logistic model using logistic equations has an upper asymptote, a ratio, and a time constant as its parameters [37]. This determines the maximum and minimum range of the model, the rate at which the growth accelerates, and the time at which the growth rate is at its maximum [38]. Until now, the logistic model has been used as the center of research to analyze growth trends using only the growth curves of crops. This characteristic of the logistic model has been exploited to analyze the crops' growth and the spread of animals, as well as to understand the effects of temperature stress [39], salinity stress [40], and pandemics [41].

The advantage of the growth curve is that the growth rate of the vegetation crop can be calculated by finding the first derivative. The growth curve of crops can be very usefully used to predict the occurrence of pests and diseases and the timing of harvest. Research using growth curves so far has been very limited. However, for vegetable crop growth, it is necessary to understand the differences by soil texture condition, as well as at what point in time the growth accelerates or slows down, and at what value the maximum is shown. The growth rate and acceleration of the Kimchi cabbage can characterize the morphology of Kimchi cabbage, and the time series of spatial variations can be used to explain the growth of Kimchi cabbage in terms of soil texture conditions.

Therefore, the purpose of this study is to (1) determine the growth variation of Kimchi cabbage according to the soil texture difference, which is the basis for growth; (2) determine the height variation of Kimchi cabbage using the RS method; (3) apply the logistic growth model to analyze the growth characteristics, growth rate, and growth acceleration of Kimchi cabbage.

## 2. Materials and Methods

### 2.1. Study Area

The study area was located in the National Institute of Agricultural Sciences (NIAS), located in Iseo-myeon, Wanju-gun, Jeollabuk-do, Korea. Figure 1 shows the study area. This study was conducted by constructing an experiment zone on the sloping field (127°02'49.65" E, 35°49'28.52" N) of NIAS. The NIAS is an institution that conducts tests and research on the agricultural environment, rural resources, biological resources, agricultural safety, agricultural energy, and production automation. The NIAS is playing a role in developing and distributing technologies related to crops that are closely related to people's lives by operating a test bed. The soil texture conditions of major Kimchi cabbage cultivation areas in Korea are mainly composed of sandy loam, loam, and clay loam. Therefore, the test bed consisted of three soil texture conditions.

### 2.2. Experimental Design

Soil is different in all locations, depending on topographical conditions, and is generally classified according to soil type. Earthiness (soil type) is divided into 12 categories according to the proportions of sand, silt, and clay. Among these, clay loam, loam, and sandy soils contain 37.5 to 50%, 25 to 37.5%, and 12.5 to 25% clay, respectively. Soils of different types have different drainage rates due to the different moisture transfer rates.

The experiment zone was divided into three treatment zones to create the soil texture conditions of loam, clay loam, and sandy loam (Figure 2). The actual cultivation area of Kimchi cabbage was 298 m<sup>2</sup> for each experimental soil texture type, with a total cultivation area of 894 m<sup>2</sup>. A total of 2031 Kimchi cabbages were cultivated in the experimental plots for each soil texture type with a size of 25.5 m × 11.7 m. The planting distance of Kimchi cabbage was 40 cm × 85 cm.

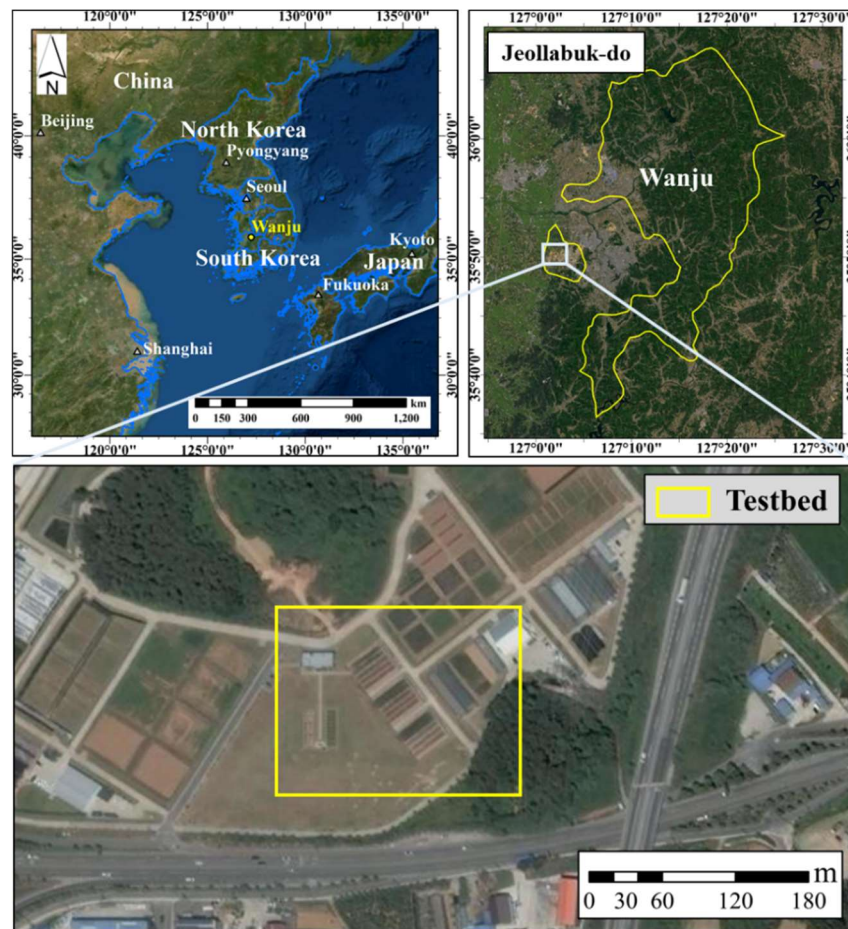


Figure 1. Study area located in the National Institute of Agricultural Sciences (NIAS), located in Iseo-myeon, Wanju-gun, Jeollabuk-do, Korea.

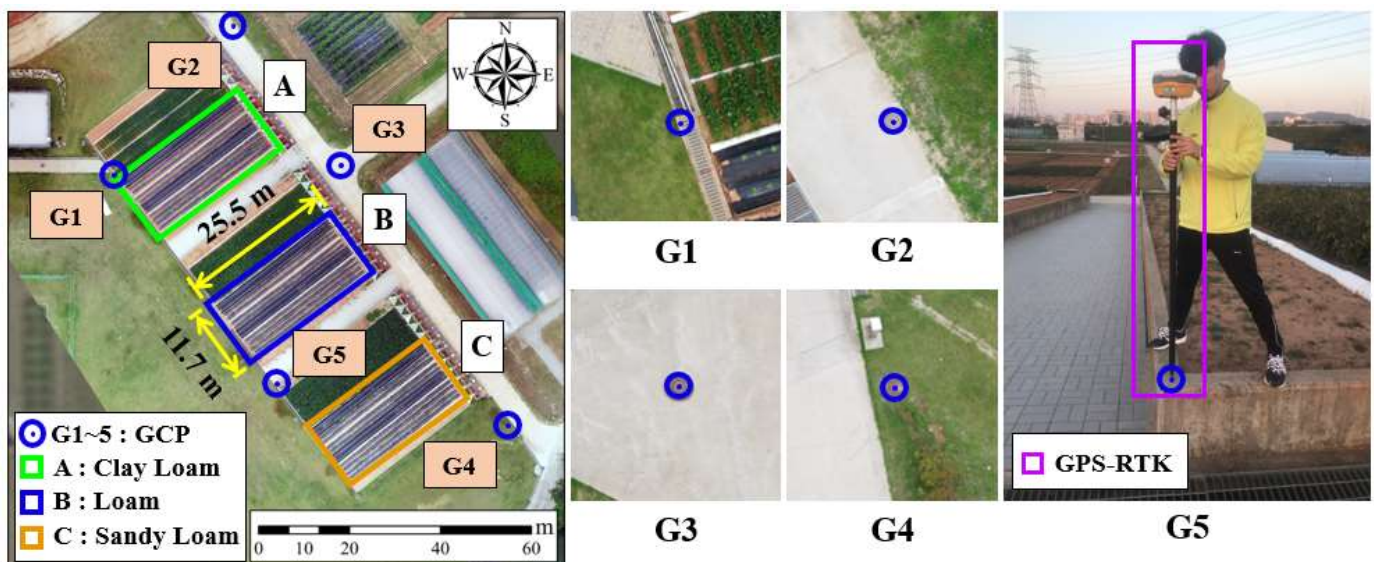


Figure 2. Kimchi cabbage experiment at NIAS and setting of field plots according to the soil texture conditions of the experimental site. G1~5 are ground control points (GCP) for measuring positioning accuracy.

Each soil texture group was assessed without irrigation in order to analyze its characteristics under natural rainfall conditions. The study was conducted by employing the

same method and conditions, and slope gradient of the plot to produce the same cultivation conditions. The cabbage variety “Autumn fairy tale” was planted on 30 August 2018 and cultivated according to the standard cultivation method.

### 2.3. Drone Image Photographing and Pre-Processing

Drone images were collected at an altitude of 30 m by mounting a Zenmuse-X5s (DJI, Shenzhen, China) sensor on a rotorcraft drone (Inspire2, DJI, Shenzhen, China). The images taken one by one were combined with the external feature data of the drone at the time of collection, and image merging and orthogonal correction were performed using a preprocessing program (Pix4D-mapper, Pix4D, Prilly, Switzerland).

To investigate the growth of Kimchi cabbage, drone images were collected from 30 August 2018, the planting date of Kimchi cabbage. The drone image photographing cycle was performed seven times at approximately 2-week intervals from 6 September 2018 to 6 November 2018. The acquired image data were RGB and DSM. The RGB image data were used to assess the situation in the field, the size and height of Kimchi cabbage, and the number of missing cabbages. DSM data were used to obtain information on the cabbage height (CH).

### 2.4. Digital Surface Model

The acquired RGB and DSM data resolutions were 0.77 cm/px and 1.1 cm/px, respectively. In the image rectification and restoration process during the pre-processing of the drone image, a DSM with a resolution of 1.1 cm and a point cloud were used to generate results with relative precision. Here, a DSM was created as a raster file in GeoTiff format and a grid file in text format, according to the input grid spacing. The detailed DSM extraction process is shown in Figure 3.

### 2.5. Cabbage Surface Model and Cabbage Height Estimation

The CSM makes it possible to estimate the CH of each cabbage by superimposing it upon the orthographic image. The CSM gives the numerical value of the surface height of cabbage (Figure 4). The CSM related to the growth stage can be extracted as in Equation (1):

$$CSM_{growth\ stage} = DSM_{growth\ stage} - DSM_{ground\ condition} \quad (1)$$

where CSM is the cabbage surface model, DSM is the digital surface model, and *growth stage* is the observation date (month/date: 9/6, 9/13, 9/27, 10/3, 10/12, 10/24, 11/6).

In a previous study [42], the coefficient of determination between the measured height and the measured value extracted with CSM was 0.948, indicating that the CSM-based construction accurately reflects the actual value. The CH value by growth stage was extracted, as in Equation (2), by subtracting the DSM of the initial vegetable-growing land from the CSM:

$$CH_{growth\ stage} = CSM_{growth\ stage} - DSM_{ground\ condition} \quad (2)$$

where  $CH_{growth\ stage}$  is the cabbage height for each growth stage,  $CSM_{growth\ stage}$  is the cabbage surface model for each growth stage, and  $DSM_{ground\ condition}$  is the numerical elevation model unique to an agricultural field without cabbages.

### 2.6. Kriging Interpolation

Kriging interpolation is a raster interpolation method that can generate a predicted surface for unmeasured points using the statistical relationships between measured points. There are various methods, such as simple Kriging, ordinary Kriging, and universal Kriging,

available for kriging interpolation. The Kriging interpolation method can obtain predicted values using weights, as in Equation (3) [43]:

$$z_0^* = \sum_{i=1}^n \lambda_i z_i \tag{3}$$

where  $z_0^*$  refers to estimated values,  $\lambda_i$  refers to weights, and  $z_i$  refers to measured values.

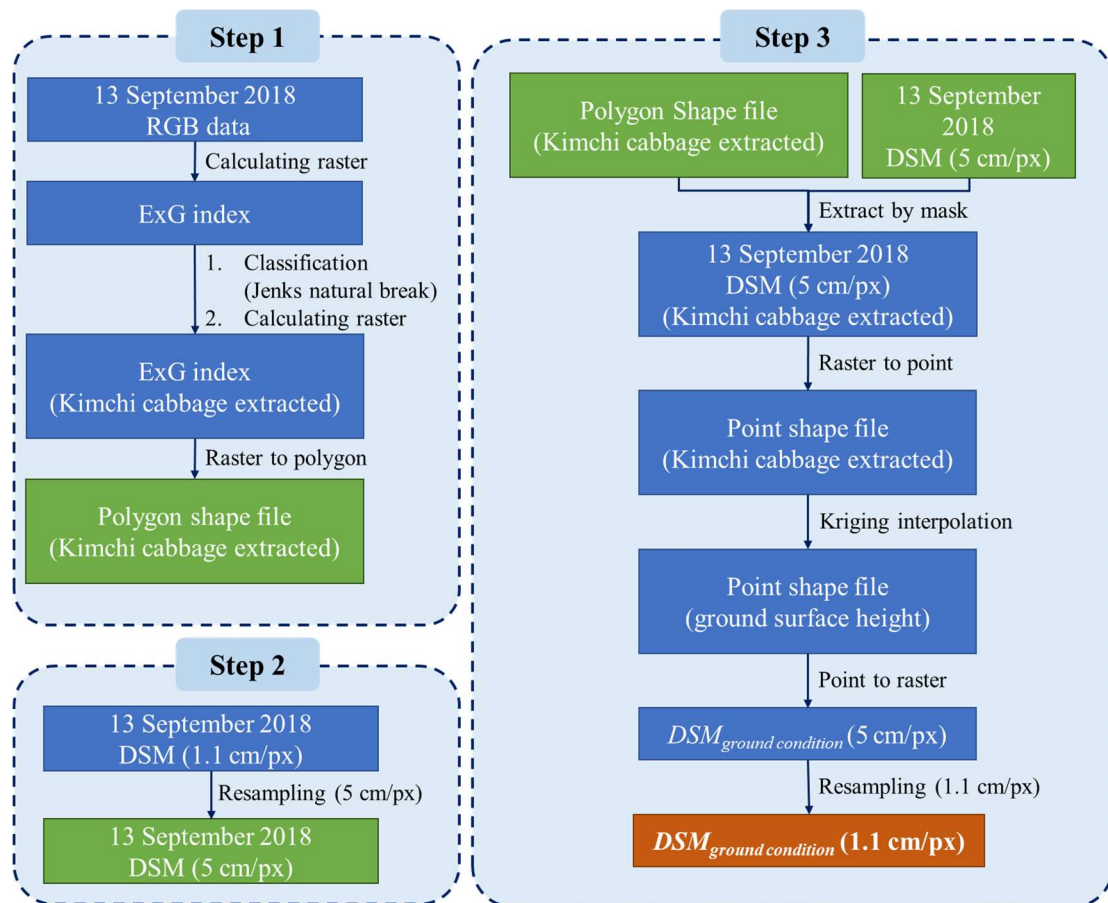


Figure 3. Workflow from image acquisition to DSM extraction.

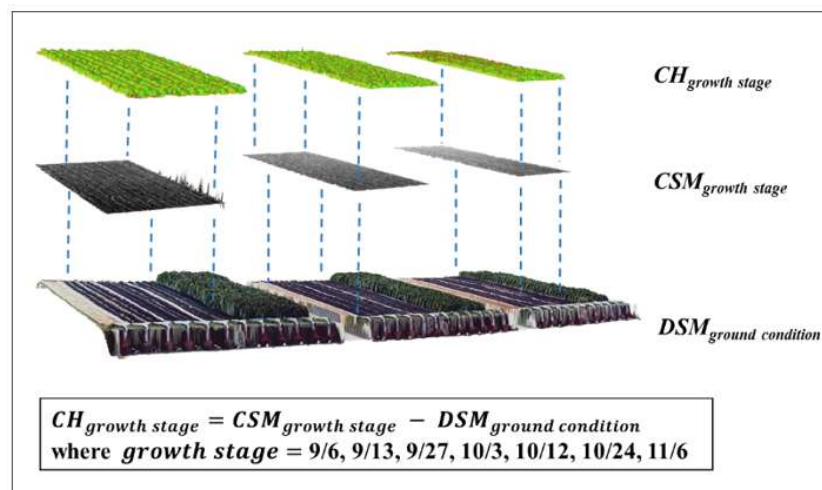
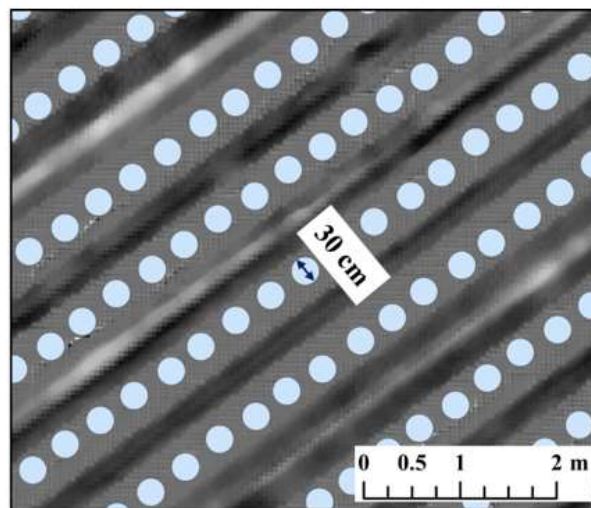


Figure 4. How to construct CH using DSM and CSM.

Ordinary Kriging is an interpolation method that minimizes error variance and has no bias estimations [43]. Therefore, the ground DSM derivation used ordinary Kriging interpolation. The initial ground DSM was derived using Kriging interpolation after removing Kimchi cabbage from the September 13th image among the acquired DSM images. Kriging interpolation improves the interpolation accuracy by reflecting not only the distance from the measured value but also the correlation strength between each neighboring value [44–46].

### 2.7. Cabbage Height Extraction for Growth Characteristics Analysis

As shown in Figure 3, the initial DSM was based on images acquired from a drone and had a raster data format. The CSM data are also in raster form since they were obtained from the DSM after the cabbage was planted.  $CH_{growth\ stage}$  was derived in the form of raster data through the calculation of  $CSM_{growth\ stage}$  and  $DSM_{ground\ condition}$ . The  $CH_{growth\ stage}$  of each Kimchi cabbage was derived by extracting the largest value from the 15 cm radius within the raster-type image data (Figure 5). The extracted  $CH_{growth\ stage}$  was used to construct a logistic growth model of Kimchi cabbage.



**Figure 5.** Height extraction range for growth characteristics analysis for each Kimchi cabbage.

### 2.8. Logistic Growth Model

In general, the growth characteristics of Kimchi cabbage are identified by measuring the increases in width, height, and weight [11]. The most common method for this is to periodically monitor and measure the time-series variation in the height of the Kimchi cabbage. As for the time-series variation in the CH, the shorter the direct observation or remote sensing measurement period, the more accurate the model implementation [47]. In order to realize such variation characteristics, in this study, the logistic model was adopted and applied.

The sigmoid function series is mathematically expressed and utilized in various ways, and the most basic and important functions are logistic [48]. Logistic functions are treated as representatives of S-shaped functions in machine learning. The growth characteristics of Kimchi cabbage vary in the form of a logistic model, and this is expressed as Equation (4):

$$G(t) = \frac{G_{max}}{1 + \left(\frac{G_{max}}{G_0} - 1\right)e^{-kt}} \quad (4)$$

where  $G(t)$  is the height of Kimchi cabbage at observation time  $t$ ,  $G_0$  represents the initial value of the height of Kimchi cabbage at observation time  $t = 0$ ,  $G_{max}$  is the maximum growth value of cabbage, and  $k$  is the initial growth rate of the cabbage.

The cabbage growth rate and acceleration formulas can be obtained via the first and second derivations, respectively, of the logistic model. The growth rate of Kimchi cabbage can be defined as a derivative of the growth curve with respect to time  $t$ , as in Equation (5):

$$V(t) = \frac{dG(t)}{dt} = kG(t) \left[ 1 - \frac{G(t)}{G_{max}} \right] \tag{5}$$

where  $V(t)$  is the rate of variation in the height of cabbage during the observation period and represents the growth rate of Kimchi cabbage.

The growth acceleration of Kimchi cabbage can be obtained by finding the derivative of the growth rate model in Equation (5). That is, the growth acceleration of Kimchi cabbage is defined as the second derivative of the growth curve with respect to time  $t$  in Equation (6):

$$a(t) = \frac{dV(t)}{dt} = \frac{d^2G(t)}{dt^2} = kV(t) \left[ 1 - \frac{2G(t)}{G_{max}} \right] \tag{6}$$

where  $a(t)$  represents the growth acceleration of Kimchi cabbage at each stage during the observation period.

### 2.9. Research Flow Process

Figure 6 shows the overall flow of this study. The cabbage growth model used in this study is a 3-parameter logistic model. Equations (4) to (6) were applied to analyze the growth characteristics, growth rate, and growth acceleration for each of the three soil textures. The model was constructed in Python version 3.8.8 (Python Software Foundation, Amsterdam, Netherlands) using the CSM value of Kimchi cabbage.

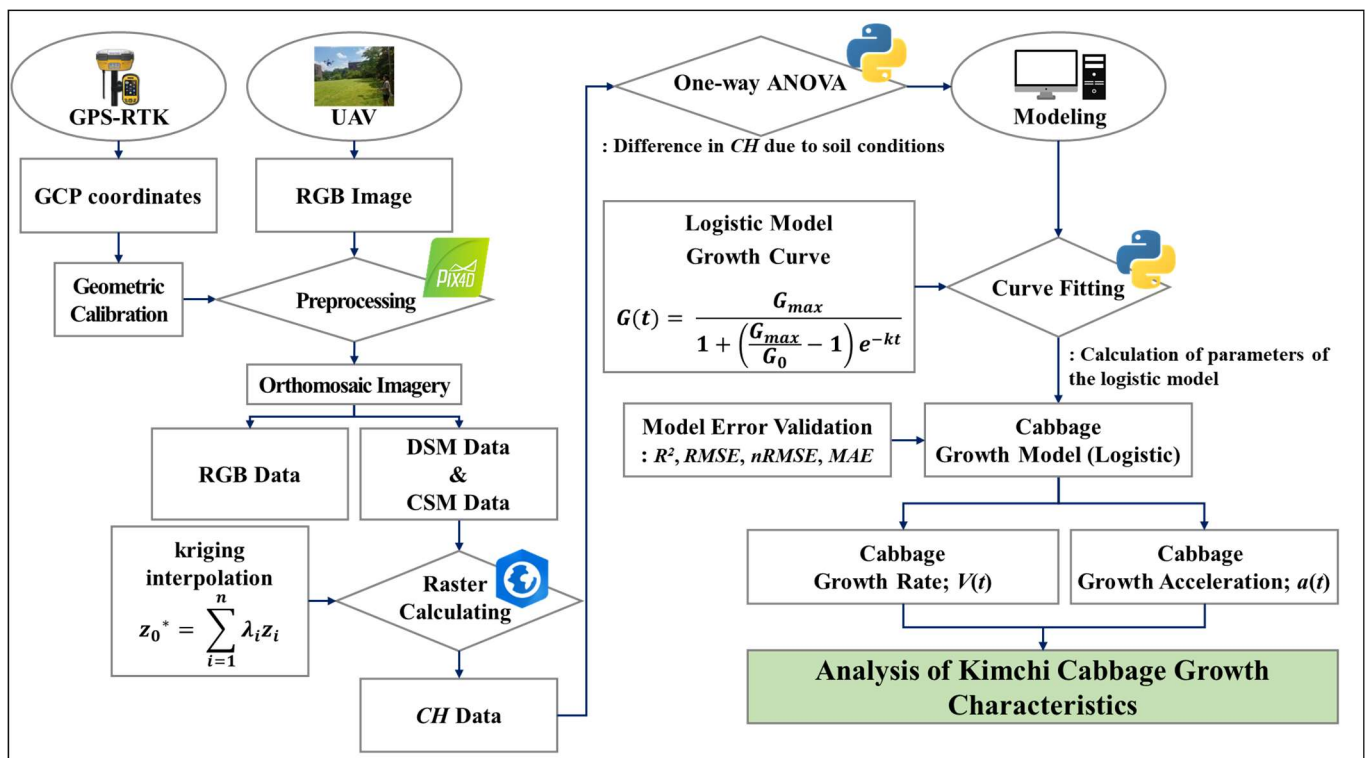


**Figure 6.** The overall research flow process from drone-based image acquisition to model application growth characteristics analysis.

The growth model was produced using the average CSM value of Kimchi cabbage according to each soil texture. In this study, the initial cabbage number were 672 clay loam, 676 loam, and 683 sandy loam by soil texture conditions. Outliers were removed using



the inter quartile range (IQR) method. The IQR method sorts the entire data in ascending order and divides it into exactly four equal parts (25%, 50%, 75%, 100%). Here, IQR is the difference between the 75% and the 25% value. This IQR is multiplied by 1.5 and added to the value at the 75% point to determine the maximum value, and subtracted from the value at the 25% point to be the minimum value. IQR outliers were removed as outliers that were greater than the determined maximum value or less than the minimum value.

The number of cabbages from which outliers were removed was 619 clay loam, 587 loam, and 606 sandy loam. From the obtained cabbage, *CH* was extracted using CSM, and the average value was calculated and used for the production of the cabbage growth curve. The production model was used to analyze the growth rate and acceleration of Kimchi cabbage by confirming the growth variation determined by soil texture, as shown in Figure 6. Accuracy evaluation of the model was performed using ANOVA,  $R^2$ , root-mean-square error (*RMSE*), normalized root-mean-square error (*nRMSE*), and mean absolute error (*MAE*).

### 2.10. Model Validation

For ANOVA analysis, one-way ANOVA, a statistical test method that compares the means between three or more groups, was used. Soil texture conditions such as clay loam, loam, and sandy loam were applied as independent variables, and CSM, a continuous variable, was used as the dependent variable. The significance of CSM by soil texture was analyzed through ANOVA analysis. ANOVA analysis was calculated using the statsmodels module in Python version 3.8.8. The significance test was based on a *p*-value of 0.05, and a post hoc test was performed to confirm the difference by soil texture. For the post hoc test, Tukey's honestly significant difference (HSD) method was used, and the CSM difference by soil texture was confirmed by conducting the test.

For verification of the constructed model, error evaluation was performed by comparing it with the CSM value of total Kimchi cabbage. Based on *CH*, a variable in cabbage growth, the accuracy was compared by employing a drone measurement value based on the square and absolute error between the drone-based value and the estimated value [49]. The *RMSE*, *nRMSE*, and *MAE* were used to compare estimation methods for the same data set:

$$RMSE = \sqrt{\frac{1}{N} \sum_{i=1}^N (\hat{p}_i - p_i)^2} \quad (7)$$

$$nRMSE = \frac{\sqrt{\sum_{i=1}^N \frac{(\hat{p}_i - p_i)^2}{N}}}{p_{\max} - p_{\min}} \quad (8)$$

$$MAE = \frac{1}{N} \sum_{i=1}^N |\hat{p}_i - p_i| \quad (9)$$

where  $\hat{p}_i$  is the measured value and  $p_i$  is the estimated value obtained by the predictive logistic model at the *i*th time step. *N* is the number of cabbages during the growing period.

## 3. Results

### 3.1. Time Series DEM Using RGB Imagery

Drone image-based DEMs are used in various ways to provide core data for the realization of precision agriculture. However, even when drone images are acquired in the same area under the same flying conditions, geometric errors occur between images due to the influence of various external factors, such as global navigation satellite system (GNSS) signals, weather conditions (such as wind), and platform posture [50].

In this study, to solve this problem, ground control points (GCPs) data, which provide absolute coordinates when producing orthographic images and DEMs, were used. The experimental field consisted of cabbages and the surrounding fixed structures that varied with time. Since the sizes and shapes of Kimchi cabbages vary according to the growing

season, the height of Kimchi cabbages is expressed differently for each period in the time-series DEM. On the other hand, the GCPs elevation does not vary, because the shapes and sizes of artificial structures (such as the ground, roads, and buildings) with no vegetation except cabbage and weeds do not change over time. Therefore, the elevation error between DEMs was corrected by analyzing the relative elevation difference in a constant region. The elevation correction of DEM was carried out by constructing a correction formula based on the elevation error and the conversion of the elevation of the DEM to which the ground reference point data were not input into the actual elevation. Elevation-invariant regions between DEMs were obtained by extracting EIFs (elevation-invariant features), which are elevation-correction data points.

Figure 7 shows the time series variations according to the Kimchi cabbage growth stage in the experimental field using drone-based RGB color images. The XY resolution of the RGB image was acquired at about 1 cm/px to produce an orthographic image, and the DSM image was extracted using the Pix4D mapper program. The growth of Kimchi cabbage is very slow for a certain seeding period after planting, so it is not easy to sort unless the RGB image is enlarged. However, the growth rate from the growth transplant period (27 September 2018) to the peak cupping and early heading period (12 October 2018) is so fast that it can be distinguished with the naked eye, so the growth difference can be confirmed. After that, growth variation classification was difficult and was characterized by slow cabbage heading variation and maturation.

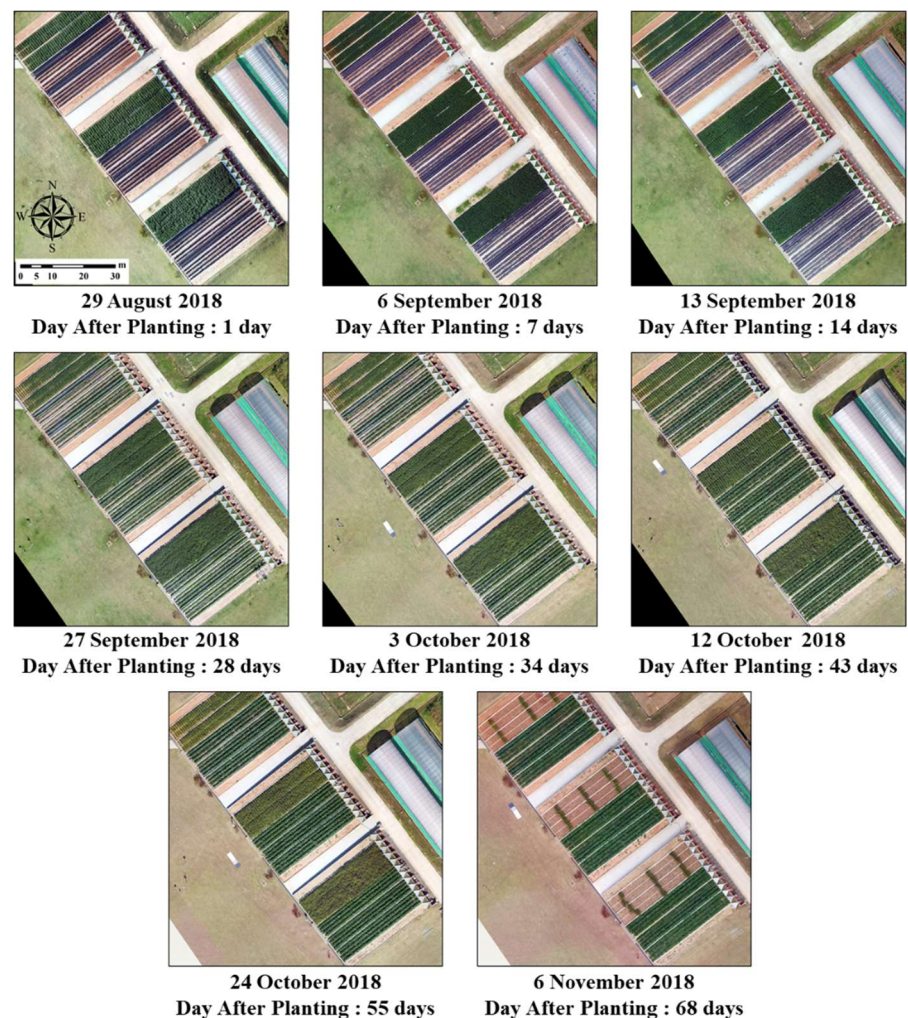


**Figure 7.** Time series variation according to the Kimchi cabbage growth stage in the experimental field using drone-based RGB color images.

In addition, it was difficult to classify the growth characteristics of each soil texture type at the initial seeding stage; it was possible to distinguish the growth difference gradually from the transplant and cupping growth stages and was difficult to classify the unique difference at the maturity stage. Therefore, it is possible to distinguish the growth characteristics of Kimchi cabbage by soil texture type with RGB color images.

### 3.2. Ground DSM Production Using Kriging Interpolation

The RGB color images collected by the drone can make the distribution of Kimchi cabbage readable with the naked eye, but it is necessary to convert these data to numerical cover in order to calculate and quantitatively evaluate the variation in vegetation. Assessing variations in vegetation cover should be preceded by the process of separating Kimchi cabbage and soil. In general, ground DSM assesses agricultural land before or after vegetable crops are planted.

The images of the experimental field plots before the cultivation of Kimchi cabbage could not be used due to an image acquisition problem, so the images after the cabbage was planted were used. The images on 29 August were taken with the Mavic's built-in camera at 1.1 cm/px. The obtained image showed severe distortion, so there was a problem with geometric correction through GCP, and a lot of errors occurred even after linear interpolation and geometric correction. The images from 6 September to 6 November were taken with the Zenmuse-X5S sensor and had a resolution of 0.77 cm/px and were acquired under conditions with very little image distortion. In this case, only soil information excluding vegetation information could be extracted.

Therefore, Figure 8b shows the ground DSM which is obtained by applying the Kriging interpolation method using ArcGIS Pro based on the RGB image (Figure 8a) acquired on 13 September. The Kriging interpolation method is a geostatistical technique that predicts the value of Kimchi cabbage not grown in the experiment zone as a linear combination of values around one that is already known. This method linearly combines the surrounding measured values for interpolation and estimates the values using the statistical method [51]. 6 September was seven days after planting, and the height of the cabbage was about 3~5 cm. Therefore, it was necessary to remove information about the height of the cabbage. The removal of vegetation information from soil information was carried out as follows. Drone-based vegetation index studies have been conducted by several researchers [47,52]. In a previous study [42,47], the ExG (Excess Green) vegetation index showed the highest accuracy in calculating the vegetation cover rate among various vegetation indexes. In this way, the vegetation and soil information of the drone image can be extracted separately by converting the RGB image to ExG and grading the histogram to obtain the Kimchi cabbage and soil boundary threshold. In this study, the Jenks natural breaks technique [52,53] was used for grading the ExG histograms. This method is mainly used to optimize the data arrangement into natural classes as a way to reduce intra-class variation and maximize inter-class variation. ExG was used to remove vegetation from the soil (Figure 8c), and the extracted DSM data were converted into points (Figure 8d) and used for topographical interpolation with Kriging interpolation to produce the ground DSM (Figure 8e).

In the process of obtaining the ground DSM, the Kriging interpolation method was inefficient when 1.1 cm/px was used. The Kriging interpolation method included the removed vegetation pixels because interpolation was performed with reference to the surrounding values in cases of super-high resolution, resulting in many errors. Therefore, points were produced and interpolated by resampling at 5 cm/px, which was not affected by the removed vegetation information pixels, with resampling at 1.1 cm/px again. As a result, the ground DSM interpolated the soil texture conditions (excluding vegetation) well and was reconstructed into a condition without vegetation. The effect of Kriging interpolation can be confirmed by extracting the center DSM of Kimchi cabbage from the DSM image before and after interpolation. The difference before and after Kriging interpolation was about 2.48 cm, confirming that the height of Kimchi cabbage was eliminated by the Kriging interpolation method (Table 1).

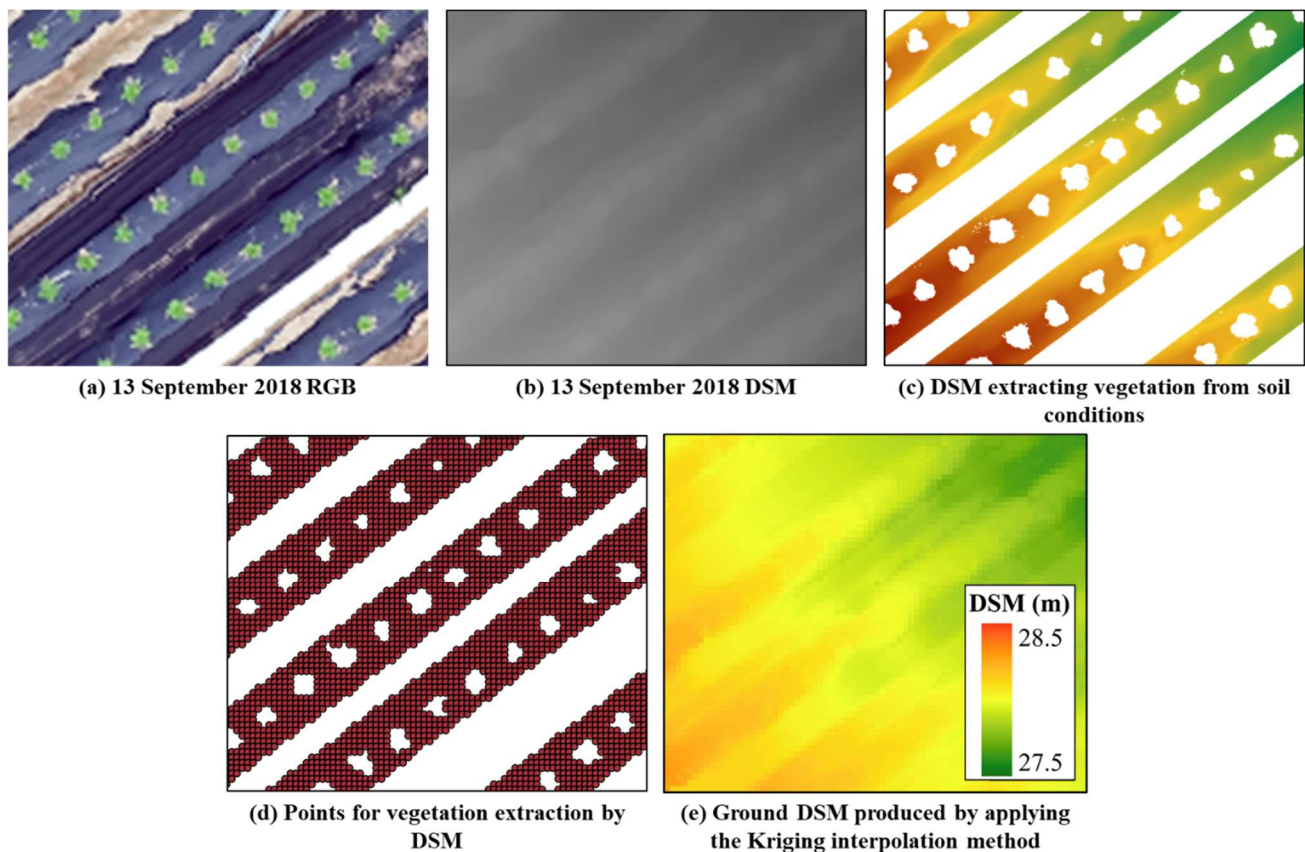


**Figure 8.** The process of constructing a ground DSM by applying the Kriging interpolation method. (a) RGB image of ground DSM extraction area. (b) An image that includes both vegetation and soil information. (c) DSM extracting vegetation from soil conditions by applying ExG histogram grading. (d) Points for vegetation extraction by DSM. (e) Ground DSM produced by applying the Kriging interpolation method.

**Table 1.** Comparison of the difference between DSM before kriging interpolation and DSM after interpolation Unit: cm.

Original DSM Mean	Kriging DSM Mean	DSM Difference Mean	DSM Difference Median	DSM Difference Standard Deviation
2790.82	2788.34	2.48	2.41	1.51

### 3.3. Establishment of the CSM for Each Soil Condition

The CSM was constructed for each stage of cabbage growth using Equation (1) after drone image preprocessing and the construction of the ground DSM. Figure 9 shows the results of CSM construction for each growth stage of Kimchi cabbage.

The CSM related to differences in soil texture conditions (clay loam, loam, sandy soil) showed the following differences. When the CSM values for each period were compared, loam was the highest, followed by sandy loam and clay loam. The height of Kimchi cabbage in each soil area was slightly greater under the conventional untreated condition, but there were no significant differences with other cover treatments. Therefore, the study was conducted following the hypothesis that treatment conditions did not affect the growth of Kimchi cabbage, but growth was strongly affected by soil texture conditions.

In the analysis, the highest value (CH) was extracted from the calculated CSM data within a radius of 15 cm from the center of the Kimchi cabbage image. One-way ANOVA was performed on the extracted CSM data to confirm the significance of the differences related to soil texture conditions. Table 2 shows the ANOVA results. The independent

variable groups for the three clay loam, loam, and sandy loam soils had a  $p$ -value of less than 0.05, indicating that there was a difference in more than one group out of the three groups. The difference between each soil texture type was tested via post hoc comparison using the Tukey HSD method.

Following post hoc comparison, Table 3 shows that the  $p$ -value for each soil texture (clay loam, loam, sandy loam) was less than 0.05, and each was different. Therefore, the growth characteristics of Kimchi cabbage were compared and reviewed for differences under each soil texture.

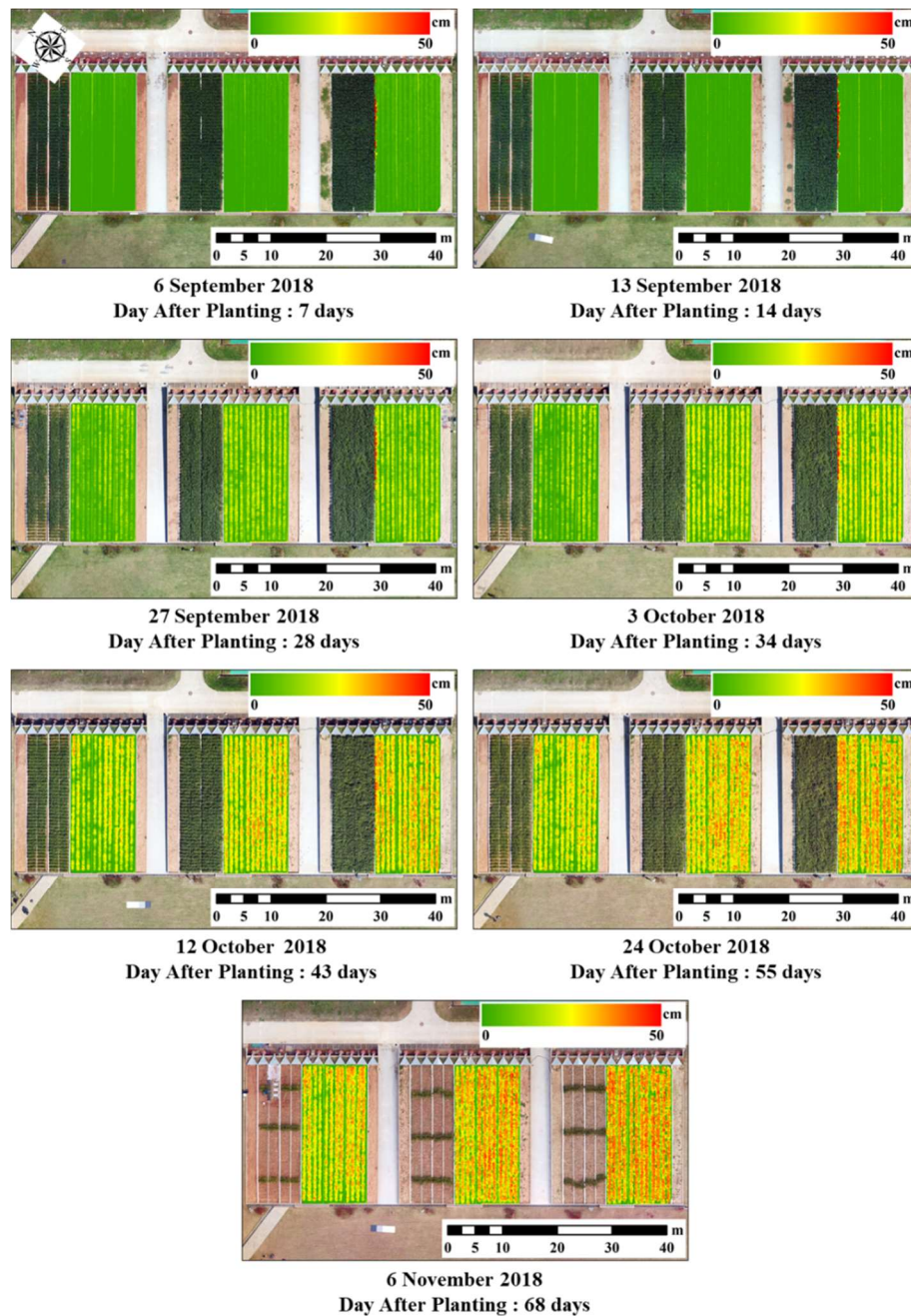


**Figure 9.** Time-series CSM variation according to the Kimchi cabbage growth stage in the experimental field using drone-based RGB color images.

**Table 2.** One-way ANOVA of soil texture type.

	df	Sum_sq	Mean_sq	F	p-Value
Soil texture	2	$7.9 \times 10^4$	39502.71	255.65	$1.61 \times 10^{-109}$
Residual	12359	$1.91 \times 10^6$	154.52	NaN	NaN

**Table 3.** Post hoc test result using the Tukey HSD method.

Group 1	Group 2	Mean Diff.	p-Adj	Lower	Upper	Reject
Clay loam	Loam	4.56	0.001	3.92	5.21	True
Clay loam	Sandy loam	5.82	0.001	5.18	6.45	True
Loam	Sandy loam	1.25	0.001	0.60	1.90	True

### 3.4. Logistic Growth Model

A growth model search was conducted for the cabbage growth trends of each soil texture. The growth trend was determined as shown in Figure 10. as a result of examining the variation in the height of Kimchi cabbage in each soil texture. As a result, the shape of the curve’s variation depended on the variation in the growing season but showed a difference based on soil texture. In the initial seeding stage, all three soil textures showed similar distributions, but the differences were evident by the later transplant stage.

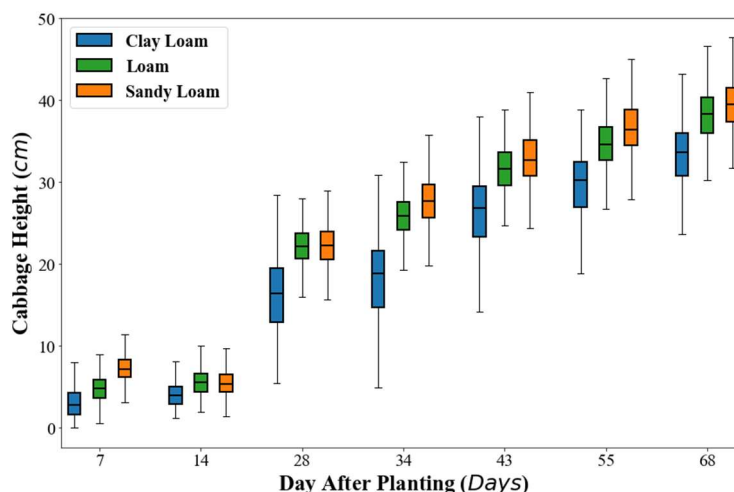


**Figure 10.** Soil-specific boxplots of the measured cabbage surface model (CSM).

Overall, as for the height distribution of Kimchi cabbage, sandy loam was the highest, followed by loam, and clay loam was the lowest. From the 28th day after seeding, the difference in the growth of each soil texture was further increased up to the transplant stage. In addition, the mean value of CSM in clay loam was lower than that in loam and sandy loam. Among the three soils, Kimchi cabbage showed the best growth in clay loam. The growth homogeneity of sandy loam and loam was similar, but clay loam showed a large difference in height.

This growth variation of Kimchi cabbage is similar to the variations in the logistic growth model. The logistic growth model was produced, as shown in Figure 11, using the CSM average value. Table 4 shows the parameter values of the produced model for the three soil textures, that is, the coefficient of determination  $R^2$ ,  $RMSE$ ,  $nRMSE$ , and  $MAE$ .

The produced logistic model is the result of comparing the CH value and the model value of all Kimchi cabbages for each soil texture at a specific date. The parameter  $G_{max}$ , which is the upper asymptote, was almost equal to the height of Kimchi cabbage in terms of the CH mean value.  $R^2$  was the lowest in clay loam, at 0.89, and it showed high regression characteristics in loam (0.95) and sandy loam (0.94).  $RMSE$  and  $MAE$  were also very low in

clay loam, about 3 cm, and loam and sandy loam value was less than 3 cm. The *nRMSE* values obtained by normalizing *RMSE* were clay loam 0.09, loam 0.06, and sandy loam 0.07, which were very low values. Therefore, the obtained results show that the logistic curve model is suitable as a Kimchi cabbage growth model.

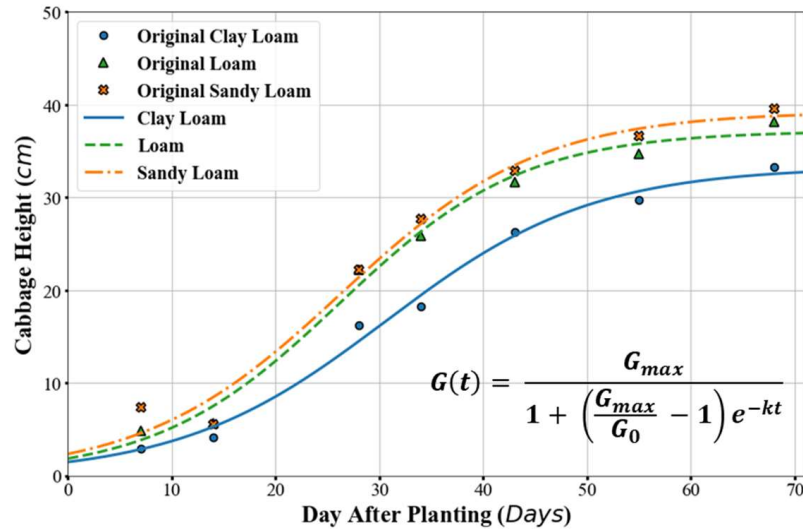


Figure 11. Logistic growth model constructed using the average value of the measured CSM and the sigmoid function.

Table 4. The parameters of the logistic growth model for three soil texture conditions.

Soil Type	$G_{max}/G_0-1$	$k$	$G_{max}$	$R^2$	<i>RMSE</i> (cm)	<i>nRMSE</i>	<i>MAE</i> (cm)
Clay loam	21.77	0.10	33.29	0.89	3.86	0.09	2.98
Loam	19.23	0.11	37.17	0.95	2.86	0.06	2.30
Sandy loam	15.82	0.11	39.25	0.94	3.13	0.07	2.59

### 3.5. Growth Rate and Acceleration of Kimchi Cabbage

The growth rate and acceleration of Kimchi cabbage were obtained through the first and second derivatives of the growth model. The obtained growth rate result is shown in Figure 12. The maximum value of the cabbage growth rate can be obtained by expressing Equation (5) as a first derivative of Equation (4).

$$\frac{dV(t)}{dG(t)} = k \left[ 1 - \frac{2G(t)}{G_{max}} \right] = 0 \tag{10}$$

$$1 - \frac{2G(t)}{G_{max}} = 0 \tag{11}$$

$$G(t) = \frac{1}{2}G_{max} = 0.5 G_{max} \tag{12}$$

The highest growth rate of Kimchi cabbage was found at  $0.5 G_{max}$ , in the order of loam 1.05 cm/day, sandy loam 1.03 cm/day, and clay loam 0.84 cm/day (Figure 12). The growth rate of Kimchi cabbage showed almost the same trend in the cases of loam and sandy loam as in the variation of the growth curve, but in the case of clay loam, it was slightly lower and showed a slow growth response. The peak growth rate ( $0.5 G_{max}$ ) was reached on the 26th day in loam and sandy loam, but the clay loam reached its peak on the 30th day, which was four days later.

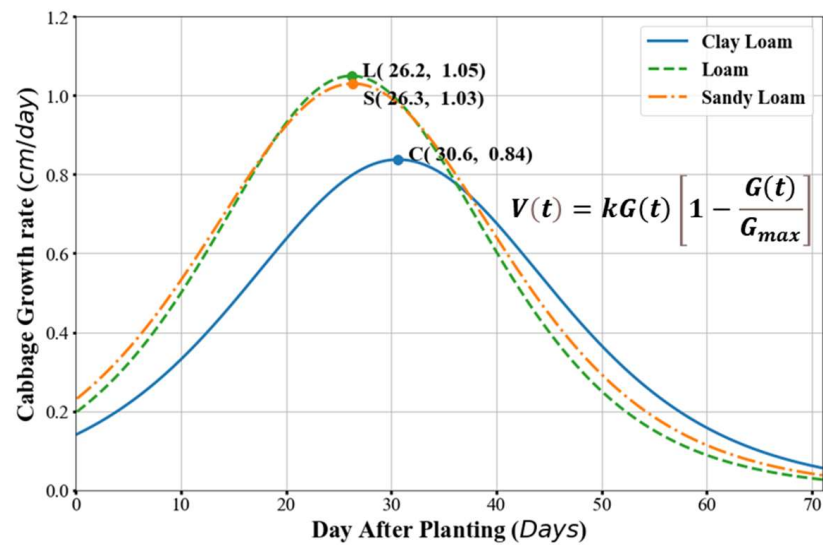


**Figure 12.** Growth rate curves of Kimchi cabbage obtained from the first derivatives of the logistic growth model.

The growth acceleration of Kimchi cabbage reached a maximum on day 14 in loam and sandy loam, but in clay loam, this was reached on day 17, i.e., three days later (Figure 13). The maximum and minimum inflection points of the cabbage growth acceleration can be obtained by expressing Equation (6) as a first derivative of Equation (4).

$$\frac{da(t)}{dG(t)} = k^2 \left[ 1 - \frac{6G(t)}{G_{max}} + \frac{6G(t)^2}{G_{max}^2} \right] = 0 \tag{13}$$

If the maximum and minimum inflection points of cabbage growth acceleration are differentiated by length, the value will be 0.

$$1 - \frac{6G(t)}{G_{max}} + \frac{6G(t)^2}{G_{max}^2} = 0 \tag{14}$$

Equation (15) is equivalent to normalization using the minimum cabbage height  $G_{min} = 0$  and the maximum height  $G_{max}$ .

$$G^*(t) = \frac{G(t) - G_{min}}{G_{max} - G_{min}} = \frac{G(t)}{G_{max}} \tag{15}$$

where  $G^*(t)$  is the normalization index for the growth curve. Substituting Equation (15) into Equation (14).

$$6G^{*2}(t) - 6G^*(t) + 1 = 0 \tag{16}$$

Equation (17) is obtained by solving the quadratic equation for Equation (16).

$$G^*(t) = \frac{G(t)}{G_{max}} = \frac{6 \mp \sqrt{6^2 - 4 \times 6 \times 1}}{2 \times 6} = \frac{3 \mp \sqrt{3}}{6} = \frac{1}{2} \mp \frac{\sqrt{3}}{6} \tag{17}$$

Therefore, the maximum and minimum values of the two inflection points of growth acceleration are as follows:

$$G(t)_L = \left[ \frac{1}{2} - \frac{\sqrt{3}}{6} \right] G_{max} = 0.2113 G_{max} \tag{18}$$



$$G(t)_U = \left[ \frac{1}{2} + \frac{\sqrt{3}}{6} \right] G_{max} = 0.7887 G_{max} \quad (19)$$

where  $G(t)_L$  is the position of the maximum value of the growth acceleration inflection point, and  $G(t)_U$  is the position of the minimum value.

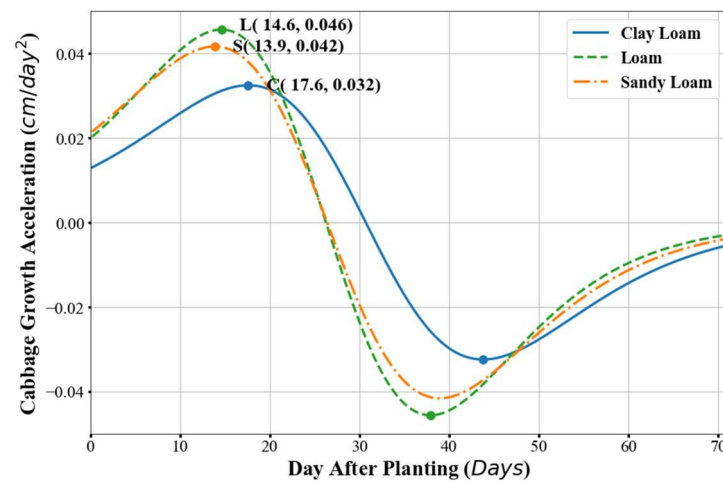


**Figure 13.** Growth acceleration curves of Kimchi cabbage obtained from the second derivatives of the logistic growth model.

#### 4. Discussion

The characteristic of this study is that drone images were used to differentiate it from the existing research on the theoretical analysis of growth characteristics of crops [1–6]. Especially, the maximum growth rate, maximum growth acceleration, and minimum values of these parameters will be useful to distinguish the growth stages of Kimchi cabbage. The section containing the maximum growth acceleration after planting ( $0.2113 G_{max}$ ) was the initial stage of slow growth, as shown in Figure 14, which corresponded to the seeding stage, and showed very slow growth. The growth during this period was affected by temperature and rainfall, so there was a noticeable difference in growth, i.e., the difference in the permeability of each soil texture is largely reflected in the growth rate and growth acceleration.

The period between the growth stage ( $0.2113 G_{max}$ ) and the maximum growth rate ( $0.5 G_{max}$ ) is the growth acceleration stage, in which the leaves of Kimchi cabbage appear and undergo rapid and high growth in a short period of time. The period between the maximum growth stage ( $0.5 G_{max}$ ) and the growth stage ( $0.7887 G_{max}$ ) is the growth deceleration stage, where the growth rate decreases and the early cupping of Kimchi cabbage occurs. After the lowest growth rate is reached ( $0.7887 G_{max}$ ), the final stage of low-speed growth begins, and the growth of cabbage almost stops; as cupping is completed, Kimchi cabbage becomes hard and reaches maturity.

As shown in Figure 14, the growth stages for each soil texture were similar in duration in the cases of loam and sandy loam. However, compared to loam and sandy loam, clay loam had the characteristics of slow growth in the initial stage, followed by a growth acceleration stage and growth deceleration stage. The difference in growth of Kimchi cabbage as determined by soil texture appeared to be due to the differences in the amounts of moisture that can be absorbed by each soil texture. The growth of Kimchi cabbage was better in soils with high permeability.

In this study, a model was produced by analyzing the growth process of Kimchi cabbage using drones and sensors, and the differences in growth rate and acceleration were analyzed. It is expected that field surveys can be conducted more scientifically and efficiently if drones and sensors are used in combination, instead of performing an actual survey, as many difficulties are encountered during field investigations.

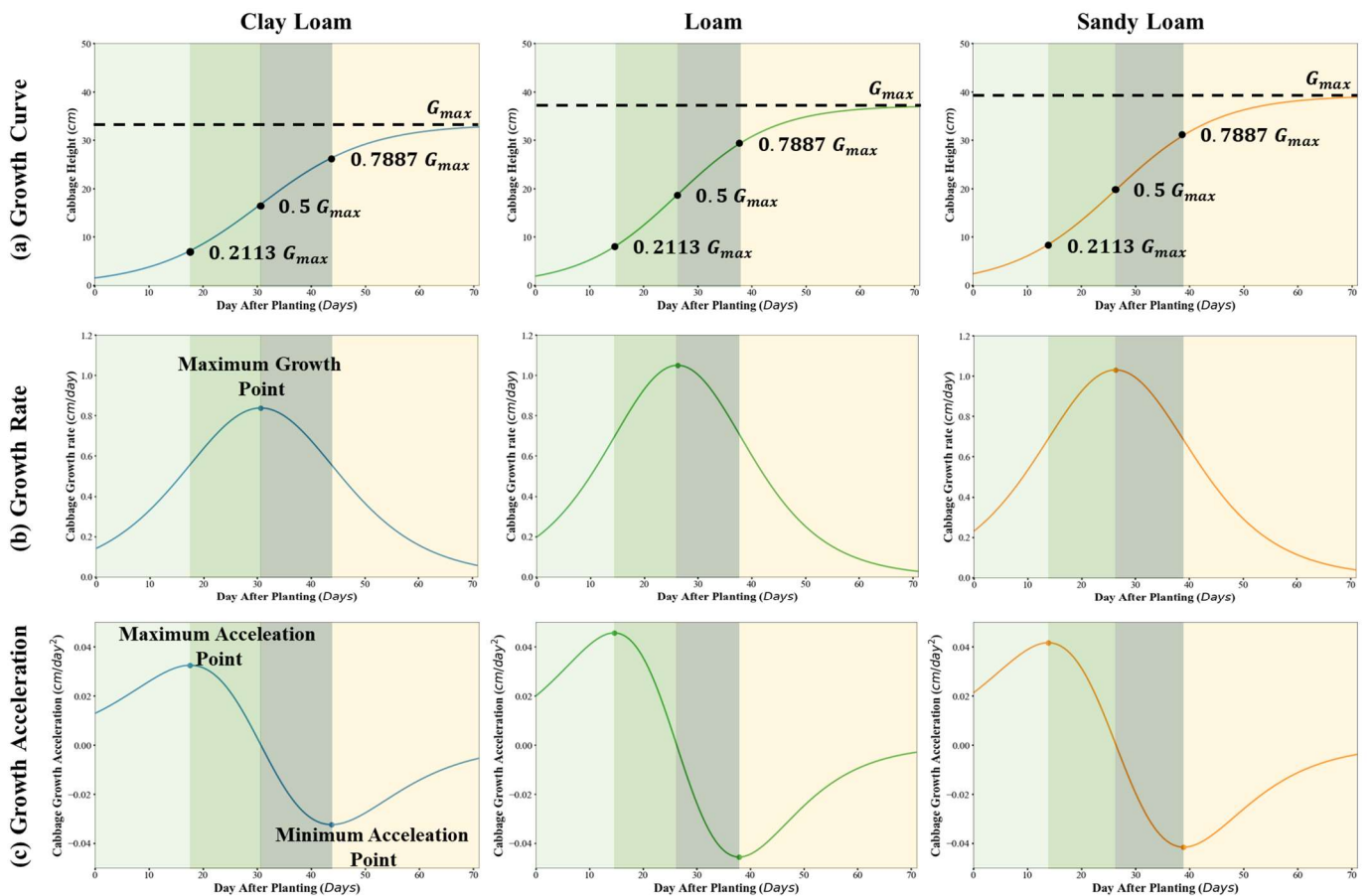


**Figure 14.** Classification of Kimchi cabbage growth stages by soil texture. (a) Logistic growth curve of Kimchi cabbage for each soil texture. (b) Growth rate curve of Kimchi cabbage. (c) Growth acceleration curve of Kimchi cabbage.

## 5. Conclusions

Accurately predicting the growth stage of Kimchi cabbage is necessary for managing the farm work schedule of growers, such as fertilizing, harvesting, and predicting the yield. In addition, this provides basic data for deriving safe, high-yielding crops under conditions of climate change in the future.

By using the variation in height according to the planting and growth of Kimchi cabbage, the growth development stage of Kimchi cabbage can be identified. The growth curve of Kimchi cabbage can be described as a logistic function. Various studies on Kimchi cabbage have been conducted so far, but none have clearly identified which point in growth is the most active and most delayed via the division of growth stages. The main factors influencing the classification of the Kimchi cabbage growth stages include the definition of the Kimchi cabbage research area, the algorithm for growth estimation, the accuracy of growth measurement, and the sample path of the growth values. This paper focused on the theoretical step division method based on drone images of the Kimchi cabbage growth process. The study was conducted on the assumption that the growth curve of Kimchi cabbage can be modeled as a logistic function. The algorithm and method proposed in this study show very high accuracy as shown in Table 4, so it can be usefully used for various crops including Kimchi cabbage.

The main conclusions obtained are as follows.

First, the growth process of Kimchi cabbage based on drone images can be divided into four stages: initial low-growth stage, high-speed growth stage, head slow-growing stage, and mature low-growth stage. The dividing points of the Kimchi cabbage growth curve were  $0.2113 G_{max}$ ,  $0.5 G_{max}$ , and  $0.7887 G_{max}$ . Here,  $G_{max}$  represents the final growth

height of Kimchi cabbage. This method can identify the growth characteristics of Kimchi cabbage and can be applied to control the growth period.

Second, in the experiments performed on the three soil texture types, it was confirmed that the growth process of Kimchi cabbage showed differences in the growth rate and acceleration depending on the soil texture. The growth rate and acceleration of sandy loam and loam were faster and greater, respectively, in the early stage than in clay loam. Compared to loam and sandy loam, the clay loam soil was characterized by slow growth. Therefore, in the clay loam, the division point of the growth stage lagged compared to the loam and sandy loam soils.

In this study, the observation of growth characteristics using drones and sensors reflected the growth characteristics of Kimchi cabbage very well. In particular, drones and sensors can be used flexibly to determine the cultivation status, as well as to objectively determine the time of planting and harvesting. In addition, the use of drones and sensors can reduce errors related to the subjective judgment of observers, such that quality information related to cabbage growth can be obtained. This highly reliable Kimchi cabbage growth stage prediction model will help to produce basic data to inform adaptation strategies in the agricultural sector under climate change scenarios.

**Author Contributions:** S.-H.G. conceived and designed the experiments; J.-H.P. conceptualized, designed the research and project administration; D.-H.L. performed the field experiments and data collection; S.-I.N. funding acquisition, resources, and validation; S.-H.G. analyzed the data and wrote the original manuscript; J.-H.P. reviewed and revised the paper. All authors have read and agreed to the published version of the manuscript.

**Funding:** This research was funded by the Cooperative Research Program for Agriculture Science & Technology Development (Project No. PJ013821042021) from the Rural Development Administration, Korea.

**Institutional Review Board Statement:** Not applicable.

**Informed Consent Statement:** Not applicable.

**Acknowledgments:** The authors thank the Rural Development Administration, Republic of Korea for their assistance during this research. We also would like to thank all of the farmers for their cooperation in this research, editors, and reviewers for their suggestions to improve the manuscript.

**Conflicts of Interest:** The authors declare no conflict of interest.

## References

- Laczi, E.; Apahidean, A.S. Protected culture study of Chinese cabbage (*Brassica campestris* var. *pekinensis*) varieties and hybrids collection grown in the Transylvanian Tableland specific conditions. *Acta Mus. Sil. Sci. Nat.* **2012**, *7*, 579–588.
- Laczi, E.; Apahidean, A.; Luca, E.; Dumitraş, A.; Boancă, P. The growth, development and yield of headed Chinese cabbage in autumn protected culture in Transylvanian Tableland specific conditions. *Agricultura* **2014**, *1/2*, 85–89. [[CrossRef](#)]
- Kalisz, A.; Cebula, S. The effect of temperature on growth and chemical composition of Chinese cabbage seedlings in spring period. *Folia Hortic.* **2006**, *18*, 3–15.
- Vavrina, C.S.; Obreza, T.A.; Cornell, J. Response of Chinese-Cabbage to Nitrogen Rate and Source in Sequential Plantings. *Hortscience* **1993**, *28*, 1164–1165. [[CrossRef](#)]
- Sammis, T.W.; Kratky, B.A.; Wu, I.P. Effects of Limited Irrigation on Lettuce and Chinese Cabbage Yields. *Irrig. Sci.* **1988**, *9*, 187–198. [[CrossRef](#)]
- Lee, S.G.; Seo, T.C.; Jang, Y.A.; Lee, J.G.; Nam, C.W.; Choi, C.S.; Yeo, K.H.; Um, Y.C. Prediction of Chinese cabbage yield as affected by planting date and nitrogen fertilization for spring production. *Prot. Hortic. Plant Fact.* **2012**, *21*, 271–275.
- Choi, H.J.; Lee, N.K.; Paik, H.D. Health benefits of lactic acid bacteria isolated from kimchi, with respect to immunomodulatory effects. *Food Sci. Biotechnol.* **2015**, *24*, 783–789. [[CrossRef](#)]
- Park, K.Y.; Kim, H.Y.; Jeong, J.K. Kimchi and its health benefits. In *Fermented Foods in Health and Disease Prevention*; Elsevier: Cambridge, MA, USA, 2017; pp. 477–502.
- Hwang, S.W.; Lee, J.Y.; Hong, S.C.; Park, Y.H.; Yun, S.G.; Park, M.H. High temperature stress of summer Chinese cabbage in alpine region. *Korean J. Soil Sci. Fert.* **2003**, *36*, 417–422.
- Larkcom, J. *Oriental vegetables: The complete guide for the gardening cook*; Kodansha USA: New York, NY, USA, 2008.
- Heo, T.W.; Il, L.C.; Hee, J.E.; Gu, A.J.; Su, K.C.; Sook, L.M. *Cabbage*; Hwang, J.H., Yoo, S.O., Kang, S.S., Eds.; Rural Department Administration (RDA): Wanju, Korea, 2020; Volume 6, p. 122.

12. Son, I.C.; Moon, K.H.; Song, E.Y.; Oh, S.J.; Seo, H.H.; Moon, Y.E.; Yang, J.Y. Effects of differentiated temperature based on growing season temperature on growth and physiological response in Chinese cabbage 'Chunkwang'. *Korean J. Agric. For. Meteorol.* **2015**, *17*, 254–260. [[CrossRef](#)]
13. Kojima, Y.; Oki, K.; Noborio, K.; Mizoguchi, M. Estimating Soil Moisture Distributions across Small Farm Fields with ALOS/PALSAR. *Int. Sch. Res. Notices* **2016**, *2016*, 4203783. [[CrossRef](#)]
14. Zhao, W.; Li, J.; Li, Y.; Yin, J. Effects of drip system uniformity on yield and quality of Chinese cabbage heads. *Agric. Water Manag.* **2012**, *110*, 118–128. [[CrossRef](#)]
15. Kim, I.G.; Park, K.J.; Kim, B.J. Analysis of meteorological factors on yield of Chinese cabbage and radish in winter cropping system. *Korean J. Agric. For. Meteorol.* **2013**, *15*, 59–66. [[CrossRef](#)]
16. Wi, S.H.; Lee, H.J.; An, S.W.; Kim, S.K. Evaluating Growth and Photosynthesis of Kimchi Cabbage According to Extreme Weather Conditions. *Agronomy* **2020**, *10*, 1846. [[CrossRef](#)]
17. Kim, K.D.; Suh, J.T.; Lee, J.N.; Yoo, D.L.; Kwon, M.; Hong, S.C. Evaluation of factors related to productivity and yield estimation based on growth characteristics and growing degree days in highland Kimchi cabbage. *Korean J. Hortic. Sci. Technol.* **2015**, *33*, 911–922. [[CrossRef](#)]
18. Zhang, X.Y.; Zhang, Q.Y. Monitoring interannual variation in global crop yield using long-term AVHRR and MODIS observations. *ISPRS J. Photogramm. Remote Sens.* **2016**, *114*, 191–205. [[CrossRef](#)]
19. Tanut, B.; Waranusast, R.; Riyamongkol, P. High Accuracy Pre-Harvest Sugarcane Yield Forecasting Model Utilizing Drone Image Analysis, Data Mining, and Reverse Design Method. *Agriculture* **2021**, *11*, 682. [[CrossRef](#)]
20. Boschetti, M.; Busetto, L.; Manfron, G.; Laborte, A.; Asilo, S.; Pazhanivelan, S.; Nelson, A. PhenoRice: A method for automatic extraction of spatio-temporal information on rice crops using satellite data time series. *Remote Sens. Environ.* **2017**, *194*, 347–365. [[CrossRef](#)]
21. Ryu, C.S.; Suguri, M.; Umeda, M. Multivariate analysis of nitrogen content for rice at the heading stage using reflectance of airborne hyperspectral remote sensing. *Field Crops Res.* **2011**, *122*, 214–224. [[CrossRef](#)]
22. Benedetti, R.; Rossini, P. On the Use of Ndvi Profiles as a Tool for Agricultural Statistics—The Case-Study of Wheat Yield Estimate and Forecast in Emilia-Romagna. *Remote Sens. Environ.* **1993**, *45*, 311–326. [[CrossRef](#)]
23. Fang, H.L.; Liang, S.L.; Hoogenboom, G.; Teasdale, J.; Cavigelli, M. Corn-yield estimation through assimilation of remotely sensed data into the CSM-CERES-Maize model. *Int. J. Remote Sens.* **2008**, *29*, 3011–3032. [[CrossRef](#)]
24. Setiyono, T.D.; Weiss, A.; Specht, J.E.; Cassman, K.G.; Dobermann, A. Leaf area index simulation in soybean grown under near-optimal conditions. *Field Crops Res.* **2008**, *108*, 82–92. [[CrossRef](#)]
25. Ballesteros, R.; Ortega, J.F.; Hernandez, D.; Moreno, M.A. Applications of georeferenced high-resolution images obtained with unmanned aerial vehicles. Part I: Description of image acquisition and processing. *Precis. Agric.* **2014**, *15*, 579–592. [[CrossRef](#)]
26. Park, J.K.; Park, J.H. Applicability evaluation of agricultural subsidies inspection using unmanned aerial vehicle. *J. Korean Soc. Agric. Eng.* **2016**, *58*, 29–37. [[CrossRef](#)]
27. Na, S.I.; Park, C.W.; Lee, K.D. Application of highland kimchi cabbage status map for growth monitoring based on unmanned aerial vehicle. *Korean J. Soil. Sci. Fert.* **2016**, *49*, 469–479. [[CrossRef](#)]
28. Weiss, M.; Jacob, F.; Duveiller, G. Remote sensing for agricultural applications: A meta-review. *Remote Sens. Environ.* **2020**, *236*, 111402. [[CrossRef](#)]
29. Park, J.K.; Park, J.H. Analysis of rice field drought area using Unmanned Aerial Vehicle (UAV) and Geographic Information System (GIS) methods. *J. Korean Soc. Agric. Eng.* **2017**, *59*, 21–28. [[CrossRef](#)]
30. Zhou, X.; Zheng, H.B.; Xu, X.Q.; He, J.Y.; Ge, X.K.; Yao, X.; Cheng, T.; Zhu, Y.; Cao, W.X.; Tian, Y.C. Predicting grain yield in rice using multi-temporal vegetation indices from UAV-based multispectral and digital imagery. *ISPRS J. Photogramm. Remote Sens.* **2017**, *130*, 246–255. [[CrossRef](#)]
31. Zheng, H.B.; Cheng, T.; Zhou, M.; Li, D.; Yao, X.; Tian, Y.C.; Cao, W.X.; Zhu, Y. Improved estimation of rice aboveground biomass combining textural and spectral analysis of UAV imagery. *Precis. Agric.* **2019**, *20*, 611–629. [[CrossRef](#)]
32. Jeong, C.H.; Park, J.H. Analysis of Growth Characteristics Using Plant Height and NDVI of Four Waxy Corn Varieties Based on UAV Imagery. *Korean J. Remote Sens.* **2021**, *37*, 733–745. [[CrossRef](#)]
33. Eom, K.C.; Song, K.C.; Ryu, K.S.; Sonn, Y.K.; Lee, S.E. Model equations to estimate the soil water characteristics curve using scaling factor. *Korean J. Soil Sci. Fert.* **1995**, *28*, 227–232.
34. Oliver, F.R. Methods of estimating the logistic growth function. *J. R. Stat. Soc.* **1964**, *13*, 57–66. [[CrossRef](#)]
35. Lee, D.H.; Shin, H.S.; Park, J.H. Developing a p-NDVI Map for Highland Kimchi Cabbage Using Spectral Information from UAVs and a Field Spectral Radiometer. *Agronomy* **2020**, *10*, 1798. [[CrossRef](#)]
36. Werker, A.R.; Jaggard, K.W. Modelling asymmetrical growth curves that rise and then fall: Applications to foliage dynamics of sugar beet (*Beta vulgaris* L.). *Ann. Bot.* **1997**, *79*, 657–665. [[CrossRef](#)]
37. Tsoularis, A.; Wallace, J. Analysis of logistic growth models. *Math. Biosci.* **2002**, *179*, 21–55. [[CrossRef](#)]
38. Birch, C.P.D. A new generalized logistic sigmoid growth equation compared with the Richards growth equation. *Ann. Bot.* **1999**, *83*, 713–723. [[CrossRef](#)]
39. Verwijst, T.; Von Fircks, H.A. Plant response to temperature stress is characterized by an asymmetric sigmoid function. *Environ. Exp. Bot.* **1994**, *34*, 69–74. [[CrossRef](#)]

40. Radanielson, A.M.; Angeles, O.; Li, T.; Ismail, A.M.; Gaydon, D.S. Describing the physiological responses of different rice genotypes to salt stress using sigmoid and piecewise linear functions. *Field Crops Res.* **2018**, *220*, 46–56. [[CrossRef](#)]
41. Vandamme, L.K.J.; De Hingh, I.H.J.T.; Fonseca, J.; Rocha, P.R.F. Similarities between pandemics and cancer in growth and risk models. *Sci. Rep.* **2021**, *11*, 1–10. [[CrossRef](#)]
42. Na, S.I.; Park, C.W.; So, K.H.; Ahn, H.Y.; Lee, K.D. Development of biomass evaluation model of winter crop using RGB imagery based on unmanned aerial vehicle. *Korean J. Remote Sens.* **2018**, *34*, 709–720. [[CrossRef](#)]
43. Yasrebi, J.; Saffari, M.; Fathi, H.; Karimian, N.; Moazallahi, M.; Gazni, R. Evaluation and comparison of ordinary kriging and inverse distance weighting methods for prediction of spatial variability of some soil chemical parameters. *Res. J. Biol. Sci.* **2009**, *4*, 93–102.
44. Park, J.K. Estimation of Rice Yield Using Artificial Neural Network (ANN) and Application of Climate Change Scenarios. Ph.D. Thesis, Chungbuk National University, Cheongju, Korea, 2014.
45. Lagueche, F.Z.B. Estimating soil contamination with Kriging interpolation method. *Am. J. Appl. Sci.* **2006**, *3*, 1894–1898. [[CrossRef](#)]
46. Zhu, Q.; Lin, H.S. Comparing Ordinary Kriging and Regression Kriging for Soil Properties in Contrasting Landscapes. *Pedosphere* **2010**, *20*, 594–606. [[CrossRef](#)]
47. Torres-Sánchez, J.; Peña, J.M.; de Castro, A.I.; López-Granados, F. Multi-temporal mapping of the vegetation fraction in early-season wheat fields using images from UAV. *Comput. Electron. Agric.* **2014**, *103*, 104–113. [[CrossRef](#)]
48. Mitchell, T.M. *Machine Learning*; McGraw Hill Education: New York, NY, USA, 1997; p. 432.
49. Calka, B.; Bielecka, E. GHS-POP Accuracy Assessment: Poland and Portugal Case Study. *Remote Sens.* **2020**, *12*, 1105. [[CrossRef](#)]
50. Xiang, H.; Tian, L. Method for automatic georeferencing aerial remote sensing (RS) images from an unmanned aerial vehicle (UAV) platform. *Biosyst. Eng.* **2011**, *108*, 104–113. [[CrossRef](#)]
51. Weber, D.D.; Englund, E.J. Evaluation and comparison of spatial interpolators II. *Math. Geol.* **1994**, *26*, 589–603. [[CrossRef](#)]
52. Dent, B.D. *Cartography: Thematic Map Design*; McGraw-Hill: Boston, MA, USA, 1999; p. 417.
53. Chen, J.; Yang, S.; Li, H.; Zhang, B.; Lv, J. Research on geographical environment unit division based on the method of natural breaks (Jenks). *Int. Arch. Photogramm. Remote Sens. Spat. Inf. Sci.* **2013**, *3*, 47–50. [[CrossRef](#)]